

Antigen 85C Inhibition Restricts *Mycobacterium tuberculosis* Growth through Disruption of Cord Factor Biosynthesis

Thulasi Warriar,^{a,*} Marielle Tropis,^b Jim Werngren,^c Anne Diehl,^d Martin Gengenbacher,^a Brigitte Schlegel,^d Markus Schade,^e Hartmut Oschkinat,^d Mamadou Daffe,^b Sven Hoffner,^c Ali Nasser Eddine,^a and Stefan H. E. Kaufmann^a

Department of Immunology, Max Planck Institute for Infection Biology, Berlin, Germany^a; Institute of Pharmacology and Structural Biology, CNRS, and University of Toulouse (Toulouse III), Toulouse, France^b; Swedish Institute for Communicable Disease Control, Solna, Sweden^c; NMR Group, Leibniz Institut für Molekulare Pharmakologie, Berlin, Germany^d; and AstraZeneca Ltd., DECS Biophysics, Macclesfield, United Kingdom^e

The antigen 85 (Ag85) protein family, consisting of Ag85A, -B, and -C, is vital for *Mycobacterium tuberculosis* due to its role in cell envelope biogenesis. The mycoloyl transferase activity of these proteins generates trehalose dimycolate (TDM), an envelope lipid essential for *M. tuberculosis* virulence, and cell wall arabinogalactan-linked mycolic acids. Inhibition of these enzymes through substrate analogs hinders growth of mycobacteria, but a link to mycolic acid synthesis has not been established. In this study, we characterized a novel inhibitor of Ag85C, 2-amino-6-propyl-4,5,6,7-tetrahydro-1-benzothiophene-3-carbonitrile (I3-AG85). I3-AG85 was isolated from a panel of four inhibitors that exhibited structure- and dose-dependent inhibition of *M. tuberculosis* division in broth culture. I3-AG85 also inhibited *M. tuberculosis* survival in infected primary macrophages. Importantly, it displayed an identical MIC against the drug-susceptible H37Rv reference strain and a panel of extensively drug-resistant/multidrug-resistant *M. tuberculosis* strains. Nuclear magnetic resonance analysis indicated binding of I3-AG85 to Ag85C, similar to its binding to the artificial substrate octylthioglucoside. Quantification of mycolic acid-linked lipids of the *M. tuberculosis* envelope showed a specific blockade of TDM synthesis. This was accompanied by accumulation of trehalose monomycolate, while the overall mycolic acid abundance remained unchanged. Inhibition of Ag85C activity also disrupted the integrity of the *M. tuberculosis* envelope. I3-AG85 inhibited the division of and reduced TDM synthesis in an *M. tuberculosis* strain deficient in Ag85C. Our results indicate that Ag85 proteins are promising targets for novel antimycobacterial drug design.

The rapid spread of drug-resistant tuberculosis (TB), mainly multidrug-resistant (MDR) and extensively drug-resistant (XDR) TB, emphasizes the urgent need for novel targets and anti-TB drugs (50, 54). *Mycobacterium tuberculosis*, the etiological agent of TB, has evolved drug resistance mechanisms through a persistent phenotype and mutations in drug target genes (13). *M. tuberculosis* invades host macrophages of infected individuals and triggers a cascade of immune mechanisms, which culminate in the formation of tuberculous granulomas in the lung (38). Most bacteria are controlled by this host response, but a fraction (i.e., dormant *M. tuberculosis*) is sustained in this antimicrobial environment, only to reactivate disease at a later time point (45). Although the currently implemented multidrug regimen is effective in curing acute disease, it may fail to completely eradicate the bacteria, particularly dormant *M. tuberculosis* (30). Moreover, prolonged anti-TB therapy over a period of 6 to 9 months frequently leads to noncompliance, which contributes to the development of MDR and XDR TB (42, 44). This dire situation demands that we gain a better understanding of TB pathogenesis, particularly for the development of effective intervention strategies.

The lipid-rich *M. tuberculosis* envelope offers numerous unique pathways critical for *M. tuberculosis* survival and serves as an attractive drug target (7). Mycolic acids are long-chain β -hydroxy fatty acids which are found in trehalose dimycolate (TDM) and trehalose monomycolate (TMM) and are covalently attached to arabinogalactan-peptidoglycan (mycolyl-AGP [mAGP]) (48). Prominent first-line drugs against TB, such as isoniazid (INH) and ethambutol (EMB), target steps in mycolic acid and arabinogalactan synthesis, respectively (6, 47, 49). Envelope mycolic acids are synthesized as TMM precursors, and the final transfer of mycolic acid from one TMM molecule to another TMM molecule generates TDM. El-

egant *in vitro* studies with purified proteins assigned this fundamental enzymatic activity to the antigen 85 (Ag85) protein family, which were initially identified as secreted immunogenic *M. tuberculosis* proteins (1, 8). Ag85A, -B, and -C, the three members of this family, share 70.8 to 77.5% sequence homology and belong to the group of α/β hydrolases (14, 35). An additional member, FbpC1 (FbpD), was proposed, but functional assays revealed the absence of mycoloyl transferase activity (22, 33). The conserved active sites point to functional redundancy of Ag85A, -B, and -C in *M. tuberculosis*, which is reflected in nonlethality of single mutants in broth culture (4, 21, 33). However, the Ag85A mutant is attenuated in host macrophages and in mice (4, 15, 21). It has also been shown that Ag85C deficiency leads to a 40% reduction in mAGP, suggesting a role of Ag85 family proteins in the synthesis of covalently linked mycolic acid (21).

The utility of Ag85 inhibitors as antimycobacterial agents has been investigated previously. Notably, 6-azido-6-deoxytrehalose (ADT) was found to inhibit all three Ag85 proteins in enzymatic assays and

Received 16 September 2011 Returned for modification 2 November 2011

Accepted 4 January 2012

Published ahead of print 30 January 2012

Address correspondence to Stefan H. E. Kaufmann, Kaufmann@mpiib-berlin.mpg.de.

* Present address: Department of Microbiology and Immunology, Weill Cornell Medical College, New York, New York, USA.

Supplemental material for this article may be found at <http://aac.asm.org/>.

Copyright © 2012, American Society for Microbiology. All Rights Reserved.

doi:10.1128/AAC.05742-11

The authors have paid a fee to allow immediate free access to this article.

has a MIC of 200 $\mu\text{g/ml}$ against *M. aurum* on solid media (8). Derivatives of 6,6'-dideoxytrehalose showed antimycobacterial activity against clinical *M. avium* isolates and the avirulent *M. tuberculosis* strain H37Ra (37). Additionally, a TDM mimic synergized with INH to inhibit *M. smegmatis* as indicated by a disk-based growth assay (53). Phosphonate inhibitors of Ag85C have been synthesized, with the most active molecules possessing a MIC range of 188 to 319 $\mu\text{g/ml}$ against *M. avium* in broth culture, with optical density (OD) as readout (20). Recently, modified enzymatic assays for high-throughput screening of Ag85 proteins have been reported (12, 19). However, Ag85 antagonists, which inhibit division of pathogenic *M. tuberculosis*, and their mechanisms of action have not yet been reported.

In this study, we analyzed a novel panel of small-molecule Ag85C binders (I1-AG85, I2-AG85, I3-AG85, and I4-AG85) identified by nuclear magnetic resonance (NMR) spectroscopy (39) (see Fig. S1 in the supplemental material). I1-AG85, isolated from a panel of 5,000 synthetic fragments, bound to purified Ag85C protein with chemical shift perturbations identical to those of the active-site binder octylthioglucoside (OSG). I2-AG85, I3-AG85, and I4-AG85 are analogs derived by substitutions on the I1-AG85 scaffold that increased antimycobacterial activity against *M. smegmatis* (39). *M. tuberculosis* growth inhibition assays in broth culture demonstrated antimycobacterial activity of all four molecules. Further, I3-AG85 limited *M. tuberculosis* replication in murine macrophages *ex vivo*. We also observed that I3-AG85 modulated *M. tuberculosis* cell wall mycolic acid specifically with regard to the TDM-TMM balance. I3-AG85 had antimycobacterial activity against the Ag85C mutant MYC1554, suggesting broad-spectrum inhibition of the Ag85 family. I3-AG85 was also active against drug-resistant *M. tuberculosis* clinical isolates, indicating a distinct mode of action. Together, these data point to the Ag85 family as relevant and promising targets for TB drug discovery.

MATERIALS AND METHODS

***M. tuberculosis* strains.** *M. tuberculosis* H37Rv (ATCC 27294) and clinical isolates MT103 and MYC1554 (Ag85C mutant) were cultured to log phase in Middlebrook 7H9 (BD Biosciences) medium with 10% albumin-dextrose-catalase (BD Biosciences), 0.2% glycerol (Sigma-Aldrich), and 0.05% Tween 80 (Sigma-Aldrich) at 37°C with shaking. Kanamycin at 35 $\mu\text{g/ml}$ was used for selection of the MYC1554 strain.

Compounds. Stock solutions of compounds (100 mM) were prepared in dimethyl sulfoxide (DMSO) (Sigma-Aldrich), and aliquots were stored at -20°C .

Mouse macrophages. Bone marrow cells were obtained from the tibiae and femora of 8- to 12-week-old female C57BL/6 mice and were differentiated into macrophages as described previously (5). The study was carried out in accordance with the German Animal Protection Law.

Resazurin assay. A rapid colorimetric redox indicator test relying on the use of a colored oxidation-reduction indicator, resazurin, was used for MIC determinations. Resazurin is commercially available as alamarBlue (AbD Serotec) in a 10 \times stock solution. A 1:1 dilution of this stock in 20% Tween 80 was prepared, and 50 μl per well (96-well plate) was added to monitor antimycobacterial activity. Compounds were diluted to working concentration ranges in 7H9 medium devoid of detergent, log-phase *M. tuberculosis* was added to the plates, and the color change of resazurin was monitored, as described previously (52). To determine the MICs of I3-AG85 against MDR and XDR *M. tuberculosis* strains, the resazurin microtiter assay (REMA), was used (31). An aliquot (30 μl) of 0.01% resazurin (Acros Organic N.V.) stock solution was added to 200 μl in each well of a 96-well plate. Reduction of the redox indicator produced a visible change of color in the medium. Strains with bacterial growth in the presence of

the test compound, compared to the drug-free growth control, were considered resistant.

[^3H]uracil assay. (i) Kinetics of *M. tuberculosis* growth *in vitro*. Compounds were diluted to working concentration ranges in 90 μl of 7H9 medium without detergent, in sextuplicates, in 96-well plates. Log-phase *M. tuberculosis* bacteria were washed once with phosphate-buffered saline (PBS) (composed of 1.06 mM monobasic potassium phosphate, 155.17 mM sodium chloride, and 2.97 mM dibasic sodium phosphate [pH 7.4]) (Gibco), and a single-cell suspension was prepared in PBS. INH, a first-line TB drug, was used as positive control at 10 μM . Bacteria were enumerated with a spectrophotometer (Novaspec; Pharmacia Biotech); an OD at 580 nm (OD_{580}) of 0.1 was equivalent to ca. 5×10^7 bacteria/ml. A sample of 10^6 bacteria in 10 μl was added to each well, and plates were incubated at 37°C. At 24 h before each time point, 1 μCi of [5,6- ^3H]uracil (Perkin-Elmer) was added to each well. After 24 h, bacilli were fixed with 10% paraformaldehyde (100 μl added to each well) and radiometric counts were measured with a Top Count NXT microplate scintillation and luminescence counter (Perkin-Elmer).

(ii) Kinetics of *M. tuberculosis* growth *ex vivo*. Mouse primary macrophages (5×10^4 /well) were plated in sextuplicates in 96-well plates in complete Dulbecco's modified Eagle's medium (DMEM) (Gibco) with 10% heat-inactivated fetal calf serum (Gibco), 5% horse serum (Gibco), 0.2 mM L-glutamine (Gibco), 10 mM HEPES (pH 6.5 to 7.5; PAA Laboratories), and 1 mM sodium pyruvate (Biochrom AG) and were incubated overnight at 37°C. Infection was performed with log-phase *M. tuberculosis*, prepared as described above, at a multiplicity of infection (MOI) of 5. After 4 h, fresh medium with the desired concentration of compound was added. Plates were pulsed with [5,6- ^3H]uracil (Perkin-Elmer) and analyzed as described above.

Lipid synthesis assay. Log-phase *M. tuberculosis* bacteria were diluted in 7H9 medium devoid of detergent such that the OD_{580} was ca. 0.01 and were incubated at 37°C until an OD_{580} of approximately 0.3 to 0.4 was reached. I3-AG85 was then added at the desired concentration, and cultures were incubated with shaking at 37°C for 48 h. Sodium [1,2- ^{14}C]acetate (Perkin-Elmer) was added at 0.5 $\mu\text{Ci/ml}$, and cultures were incubated for an additional 24 h with shaking at 37°C. Lipid extraction was performed as described previously (10). Extractable lipids containing TDM, TMM, and free mycolic acids were run on silica gel-coated G-60 plates with chloroform-methanol-water (30:8:1) to separate TDM and TMM bands and with chloroform-methanol (9:1) to identify free mycolic acids. Mycolic acid methyl esters (MAME) were extracted from mAGP on delipidated bacilli by standard protocols and were run with petroleum ether-diethyl ether (9:1) four times to observe mAGP MAME. The complete bacterial pellet was autoclaved, and MAME were extracted and were run with petroleum ether-diethyl ether (9:1) to visualize total cell MAME. Quantification was performed using Typhoon 9400 imaging (GE Healthcare) and ImageQuant software (GE Healthcare).

Permeability assay. Log-phase *M. tuberculosis* bacteria were diluted in 7H9 medium without detergent to obtain 10^7 bacteria per ml. I3-AG85 was added at 100 μM , and cultures were incubated at 37°C for 48 h with mild shaking. One microcurie of [5,6- ^3H]uracil was added to each culture and incubated at 37°C for an additional 24 h. The cell pellet was suspended in 1 ml PBS, and 100 μl was collected to measure radiometric counts to enumerate cell numbers as a normalizing factor. Remnant cells were centrifuged and suspended in 600 μl of PBS. Two microcuries of [U- ^{14}C]glycerol (Perkin-Elmer) was added to each sample, and the cell pellet was collected, snap-frozen on dry ice, and fixed immediately with 10% paraformaldehyde (time zero). Similarly, samples were collected at 2, 6, 10, 15, and 20 min after addition of glycerol. Radiometric counts were measured and normalized, first to the cell numbers as measured by ^3H counts and then to untreated sample(s), taken as 1.

NMR studies. (i) Recombinant expression of Ag85A, -B, and -C. Plasmids for expression of Ag85A (NP_338463.1; amino acids 62 to 355) and Ag85B (NP_336393.1; amino acids 91 to 374) (pQE80L derivatives) were kindly provided by Kris Huygen (WIV Pasteur Institute, Brussels,

Belgium). Plasmid pMRLB16 (pET22b-Ag85C) for the expression of Ag85C (NP_334547.1; amino acids 53 to 346) was obtained from BEI Resources. Ag85 variants were cloned without signal peptides. The Ag85A and -B constructs carry an N-terminal His tag, and the Ag85C construct carries a C-terminal His tag (see Fig. S2 in the supplemental material). Expression and purification of proteins were performed as described in the supplemental material.

(ii) **Binding studies by NMR.** Binding of I3-AG85 or OSG to Ag85A, -B, and -C was monitored by two series of ^{15}N - ^1H heteronuclear single-quantum correlation spectroscopy (HSQC) experiments using either (i) PBS buffer with 0.5% DMSO at pH 7.0 or (ii) 5 mM citrate buffer (pH 6.0) containing 1 mM dithiothreitol (DTT), 0.5% DMSO, and 0.1% 3-[(3-cholamidopropyl)-dimethylammonio]-1-propanesulfonate (CHAPS) to achieve better resolution. With Ag85C, an additional experiment was performed with the latter buffer modified using 5% DMSO to generate results comparable to those obtained by Scheich et al. (39). The protein concentration was 30 μM . The compounds were added from a stock solution in DMSO to yield a concentration of 600 μM and a DMSO concentration of 0.5%. All measurements were performed at 300 K using 5-mm sample tubes and 10% D_2O in the buffer. Spectra were recorded on a Bruker AVIII 600-MHz spectrometer using a 5-mm inverse triple resonance (TCI) probe equipped with a one-axis shielded gradient. ^{15}N - ^1H HSQC spectra were recorded using Watergate water suppression, 250 scans, and 512×64 complex points (11, 28, 32). Spectral widths were 3,012 Hz and 10,000 Hz and in F_1 and F_2 , respectively. Raw data were processed with Topspin 3.1 (Bruker, Karlsruhe, Germany). A squared cosine window function was applied in F_1 and a Lorentz-to-Gauss window in F_2 . Zero filling yielded a final data matrix of $4,096 \times 2,048$ complex points. Spectra were referenced externally to 4,4-dimethyl-4-silapentane-1-sulfonic acid (DSS) (^1H) and liquid ammonia (^{15}N).

RESULTS

Ag85C inhibition restricts *M. tuberculosis* growth. The MICs of the Ag85C inhibitors I1-AG85, I2-AG85, I3-AG85, and I4-AG85 were evaluated against *M. tuberculosis* cultured in 7H9 broth, using the standard resazurin assay. Resazurin, a blue dye, is reduced to pink resorufin by respiratory enzymes in live cells. Thus, inhibition of this color change indicates impaired *M. tuberculosis* division (52). The starting structure, 2-amino-cyclohepta[*b*]thiophene-3-carbonitrile (I1-AG85), displayed negligible *M. tuberculosis* growth inhibition, with inhibitory concentrations of 1.3 mM and above (Fig. 1A). The analogs, I2-AG85, I3-AG85, and I4-AG85, had lower MICs of 250, 100, and 50 μM , respectively (Fig. 1A).

Incorporation of radioactive uracil during *M. tuberculosis* multiplication was monitored to determine antimycobacterial activity of the analogs over a period of 120 h. Radiometric counts per minute directly correlate with the number of bacteria during active replication (9). I3-AG85 was the most active analog, since 250 μM I3-AG85 was sufficient to reduce uracil incorporation by 99% after 120 h of incubation (Fig. 1B). Moreover, as early as 24 h postincubation, the reduced uracil counts observed indicated growth inhibition. On the other hand, I2-AG85 displayed 85% reduction in uracil incorporation only at 250 μM , while I4-AG85 showed similar activity at all concentrations after 120 h of incubation with *M. tuberculosis* (Fig. 1B).

During infection, *M. tuberculosis* is taken up by macrophages, where it actively replicates (16). Hence, we tested I2-AG85, I3-AG85, and I4-AG85 in *ex vivo* infection assays with mouse bone marrow-derived macrophages. Nontoxic concentration ranges were first determined with a colorimetric cell viability assay using 3-(4,5-dimethylthiazol-2-yl)-2,5-diphenyltetrazolium bromide (MTT), a yellow tetrazole (see Fig. S3 in the supplemental material) (29). Primary macrophages were infected with log-phase bac-

teria at an MOI of 5, and compounds were added to the medium after 4 h of infection. The effects of the compounds on internalized *M. tuberculosis* within macrophages were evaluated by the [^3H]uracil incorporation assay. Only I3-AG85 reduced survival of *M. tuberculosis* inside macrophages and at a 100 μM concentration (Fig. 1C).

I3-AG85 is active against MDR and XDR *M. tuberculosis* strains. Next, we investigated whether I3-AG85 could inhibit the growth of drug-resistant *M. tuberculosis* strains. MDR and XDR TB are serious public health problems in numerous parts of the world (34). A panel of 7 MDR and 3 XDR *M. tuberculosis* strains, originating from different parts of the globe and resistant to a spectrum of current first- and second-line TB drugs, were exposed to I3-AG85 (Table 1). The standard REMA revealed a MIC of 200 μM or lower for I3-AG85 against all 10 strains tested, which was indistinguishable from that against the drug-susceptible reference strain, H37Rv (MIC of 200 μM) (Table 1) (26, 41). This result suggests a mode of action that differs from those of the antibiotics that are ineffective against the tested *M. tuberculosis* strains.

I3-AG85 inhibits TDM synthesis. Mycolic acid-containing lipids generated by Ag85 proteins were analyzed in *M. tuberculosis* after I3-AG85 exposure. As a first step, TDM and mAGP syntheses were assessed. To measure the amounts of TDM and TMM synthesized during compound exposure, log-phase cultures of *M. tuberculosis* were incubated with 50 μM and 100 μM compound or without compound for 48 h. [^{14}C]acetate was then added to label the lipid fraction, and crude lipid extracts were obtained after 24 h. The extracts were separated by thin-layer chromatography with chloroform-methanol-water at a ratio of 30:8:1 as the solvent on a silica gel matrix. The intensities of the observed TDM and TMM bands were quantified.

The TDM band intensity was reduced by 15% at a 100 μM concentration of I3-AG85, while the TMM intensity increased to 125 or 200% at an I3-AG85 concentration of 50 or 100 μM , respectively (Fig. 2A). Unexpectedly, free mycolic acids also showed an increase to 200% of the untreated level at 100 μM (Fig. 2A). On the other hand, mAGP-derived MAME remained unchanged, suggesting a specific effect on TDM synthesis (Fig. 2B). I3-AG85 did not modify mycolic acid synthesis, as total cell-derived MAME were similar to those in untreated controls (Fig. 2B). I3-AG85 thus perturbed the TDM-TMM balance.

The mode of action of I3-AG85 was distinct from that of INH, which targets the earlier FASII-mediated mycolic acid synthesis step during *M. tuberculosis* lipid biogenesis (25). The drastic reduction of TDM, TMM, mAGP-MAME, and total MAME amounts with 10 μM INH exposure supports this suggestion (Fig. 2A and B). It could also explain I3-AG85 activity against INH-resistant MDR and XDR *M. tuberculosis* strains (Table 1).

I3-AG85 modulates cell envelope integrity. TDM and TMM are localized in the outer, noncovalently attached layer of the mycobacterial cell wall. These mycolic acid-containing lipids are essential for maintenance of this structure and its limited permeability (18). Differential TDM-TMM abundance induced by I3-AG85 could lead to changes in envelope integrity. To measure this, the accumulation of radioactively labeled glycerol over 20 min was monitored in bacteria pretreated with 100 μM I3-AG85 (23). Glycerol is a small, hydrophilic source of carbon that is taken up by both passive diffusion and active transport. A 30% increase in uptake of glycerol was observed, which suggests modification of *M. tuberculosis*'s envelope organization (Fig. 2C). Mild perturba-

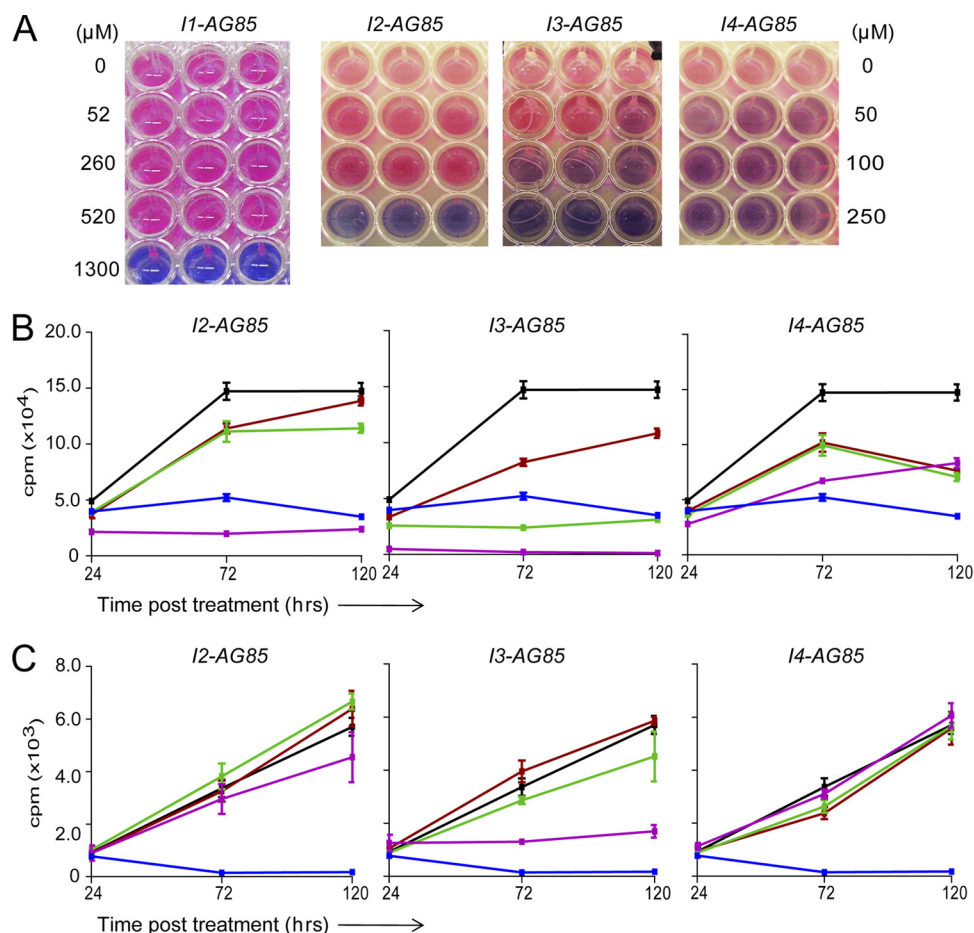


FIG 1 *M. tuberculosis* Ag85C antagonists inhibit *M. tuberculosis* growth in broth culture. (A) Log-phase *M. tuberculosis* organisms diluted in 7H9 medium without detergent were treated with indicated concentrations of compounds, I1-AG85, I2-AG85, I3-AG85, and I4-AG85. AlamarBlue ($1\times$ final concentration) was added after 96 h of incubation with compounds, and the color change was monitored after 24 h. Pink indicates live bacteria, while blue indicates dead bacteria. The figure is representative of three independent experiments. (B) Log-phase *M. tuberculosis* organisms were incubated with 50 μM (magenta), 100 μM (green), or 250 μM (pink) of I2-AG85, I3-AG85, or I4-AG85, with isoniazid (INH) at 10 μM (blue), or without compound (black) in 7H9 medium without detergent for 120 h. At 24 h prior to each time point, 1 μCi of [^3H]uracil was added to each sample, and incorporation was measured after fixation, harvesting, and measurement of cpm. cpm is plotted against duration of exposure. Means \pm standard deviations from sextuplicates in a representative experiment, from two independent experiments, are shown. (C) Primary mouse macrophages derived from bone marrow of C57BL/6 mice were infected with log-phase *M. tuberculosis* organisms at a multiplicity of infection of 5. After 4 h of infection, cells were incubated with 10 μM (magenta), 50 μM (green), or 100 μM (pink) of I2-AG85, I3-AG85, or I4-AG85, with INH at 100 $\mu\text{g/ml}$ (blue), or without compound (black). [^3H]uracil incorporation by *M. tuberculosis* was measured as described above. Means \pm standard deviations from sextuplicates in a representative experiment, from two independent experiments, are shown.

tion of the *M. tuberculosis* envelope by I3-AG85 treatment could result in uncontrolled diffusion leading to bacterial death.

An Ag85C mutant is susceptible to I3-AG85. I3-AG85 specificity was investigated by measuring susceptibility of an *M. tuberculosis* strain (MYC1554) deficient in Ag85C (21). The resazurin assay indicated inhibition of MYC1554 and its wild-type background strain, MT103, by I3-AG85 at and above 100 μM (Fig. 3A). This was mirrored in the uracil incorporation assay (Fig. 3B).

TDM and TMM band intensities were also analyzed after exposure of MYC1554 and MT103 to 100 μM I3-AG85. As with H37Rv, TDM was reduced by up to 20% in MT103, while in MYC1554 there was a larger reduction of 40% (Fig. 3C). However, there was no significant accumulation of TMM but a 4-fold increase in free mycolic acids (Fig. 3C).

I3-AG85 binds to Ag85C. I1-AG85 binding to Ag85C has been

demonstrated by recent NMR studies (39). Here, the binding of the derivative I3-AG85 to Ag85C was investigated by ^{15}N - ^1H HSQC using three different buffer systems containing different amounts of DMSO or including/excluding CHAPS (see Materials and Methods). The spectrum of Ag85C with I3-AG85 showed peak shifts caused by compound binding in comparison to the spectrum without ligand (Fig. 4A). These binding studies were performed in citrate buffer with CHAPS and a low DMSO concentration (0.5%), compatible with the MIC assays (Fig. 1) in which DMSO concentrations of 0.1 to 0.25% were used. Ag85C also showed chemical shift changes with OSG, again concordant with published results (Fig. 4B) (39). The interaction of Ag85C with OSG and I3-AG85 was also observed in physiological PBS buffer at pH 7.0 with a low DMSO concentration of 0.5% but without the detergent CHAPS (see Fig. S4A and B in the supple-

TABLE 1 Activity of I3-AG85 against drug-resistant *Mycobacterium tuberculosis*

Strain ^a	MIC (μ M)	Drug resistance profile ^b
XTB-09-036 (XDR)	200	INH, RIF, EMB, AMK, KAN, CAP, STR, OFL, RFB, ETH, PAS
BTB-06-191 (XDR)	200	INH, RIF, EMB, AMK, KAN, CAP, OFL, MXF, ETH, PAS
XTB-09-105 (XDR)	200	INH, RIF, EMB, AMK, KAN, CAP, STR, OFL, RFB, ETH, PAS
XTB-09-035 (MDR)	100	INH, RIF, EMB, AMK, KAN, CAP, STR, RFB, PAS
XTB-09-037 (MDR)	200	INH, RIF, EMB, AMK, KAN, CAP, STR, RFB, PAS
XTB-09-106 (MDR)	200	INH, RIF, EMB, AMK, KAN, CAP, STR, RFB, PAS
XTB-09-108 (MDR)	200	INH, RIF, EMB, CAP, STR, RFB, CS, PAS
BTB-09-086 (MDR)	100–200	INH, RIF, EMB, RFB, PAS
BTB-08-309 (MDR)	100–200	INH, RIF, RFB, PAS
BTB-08-325 (MDR)	100–200	INH, RIF, EMB, RFB, PAS
H37Rv	200	Pansusceptible

^a MDR, multidrug resistant; XDR, extensively drug resistant.

^b AMK, amikacin; CAP, capreomycin; CS, cycloserine; EMB, ethambutol; ETH, ethionamide; INH, isoniazid; KAN, kanamycin; MXF, moxifloxacin; OFL, ofloxacin; PAS, *para*-amino salicylic acid; RFB, rifabutin; RIF, rifampin; STR, streptomycin. The drug resistance profile was determined by standard reference techniques, i.e., the proportion method on Lowenstein-Jensen medium for PAS and CYC and the MGIT 960 system (Becton & Dickinson) for the rest of the substances (41).

mental material). The chemical shift changes observed upon addition of OSG were always stronger than those for I3-AG85.

The crystal structures of Ag85A, -B, and -C reveal nearly identical catalytic sites around the serine nucleophile and high structural conservation at the carbohydrate binding site (2, 35, 36) (Fig. 4E). Hence, NMR binding assays were performed with the two homologs Ag85A and -B. Minimal peak shifts were observed in the spectra of Ag85A with I3-AG85 (Fig. 4C), and there were some effects of line broadening. Raising the DMSO concentration to 5% to ensure I3-AG85 solubility or using physiological PBS buffer at pH 7.0 did not enhance the effect (see Fig. S5A and B in the supplemental material). OSG did bind to Ag85A when CHAPS in citrate buffer at pH 6.0 was used (Fig. 4D). However, few chemical shift changes were observed under physiological buffer conditions (see Fig. S5C in the supplemental material). Ag85B did not interact with I3-AG85 or OSG (see Fig. S6A and B in the supplemental material).

The binding patterns of Ag85 cognates with I3-AG85 are distinct, suggesting that I3-AG85 is highly specific for Ag85C, since it binds only weakly to Ag85A and not to Ag85B. This can be attributed to the presence of critical aromatic residues (F150 and W158) in Ag85C that could aid binding to the lipid moiety of OSG and, presumably, to the aliphatic chain of I3-AG85 (Fig. 4E).

DISCUSSION

Historically, the bacterial cell wall has been a preferred target for development of antibiotics, as exemplified by β -lactams, cephalosporins, and glycopeptides (40). The mycobacterial cell envelope has been the subject of extensive research, primarily due to its unique chemical components, such as the 70- to 90-carbon-atom mycolic acids (17). Ag85 proteins catalyze the pivotal mycoloyl transfer reaction in *M. tuberculosis* envelope biogenesis. We have

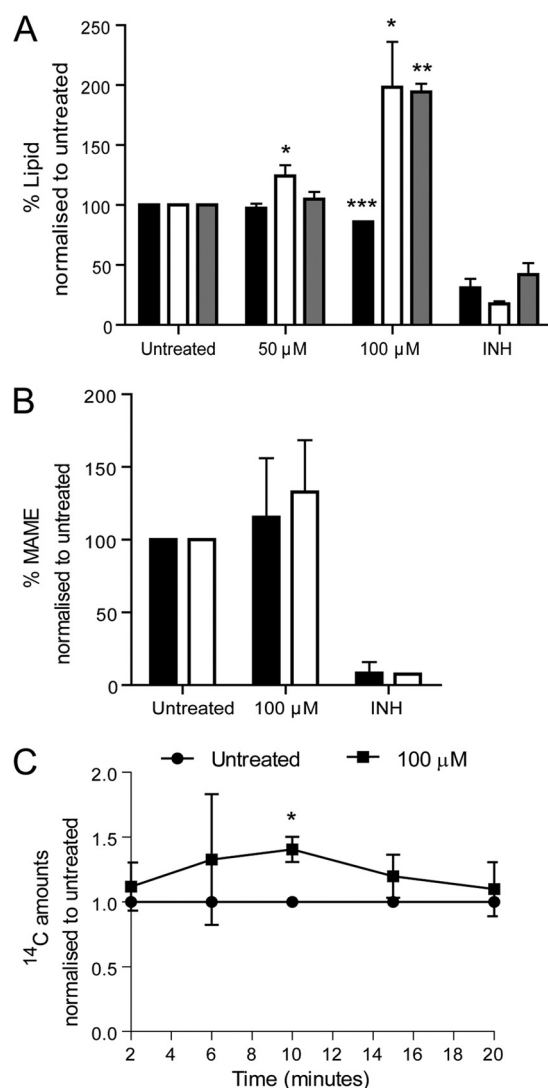


FIG 2 I3-AG85 modifies TDM-TMM and perturbs the *M. tuberculosis* envelope through Ag85 blockade. Log-phase *M. tuberculosis* bacilli exposed to the indicated concentration of I3-AG85 or 10 μ M isoniazid (INH) were pulsed with [¹⁴C]acetate to label lipids. (A) Extractable lipids were resolved by thin-layer chromatography (TLC), and the band intensities for trehalose dimycolate (TDM) (black bars), trehalose monomycolate (TMM) (white bars), and free mycolic acid (gray bars) were measured and normalized to total lane intensity. This was then converted to a percentage, with the value for untreated cells taken as 100%. Means \pm standard deviations from three independent experiments are shown. (B) Mycolyl-arabinogalactan-peptidoglycan (mAGP) mycolic acids (black bars) or total mycolic acids (white bars) were extracted from the surface of delipidated bacteria and total bacterial pellet, respectively. After conversion to methyl esters (MAME), samples were resolved by TLC to yield distinct MAME bands. The total MAME band intensity was measured and normalized to the total lane intensity. It was then converted to a percentage, with the value for untreated cells taken as 100%. Means \pm standard deviations from three independent experiments are shown. (C) I3-AG85-treated (■) or untreated (●) *M. tuberculosis* bacilli were incubated with [¹⁴C]glycerol, and radiometric counts in the bacterial pellet were measured over 20 min. This was first normalized for number of bacteria and then normalized to untreated cells, taken as 1. Statistical significance was calculated with the paired Student *t* test: *, *P* < 0.05; **, *P* < 0.01; ***, *P* < 0.001.

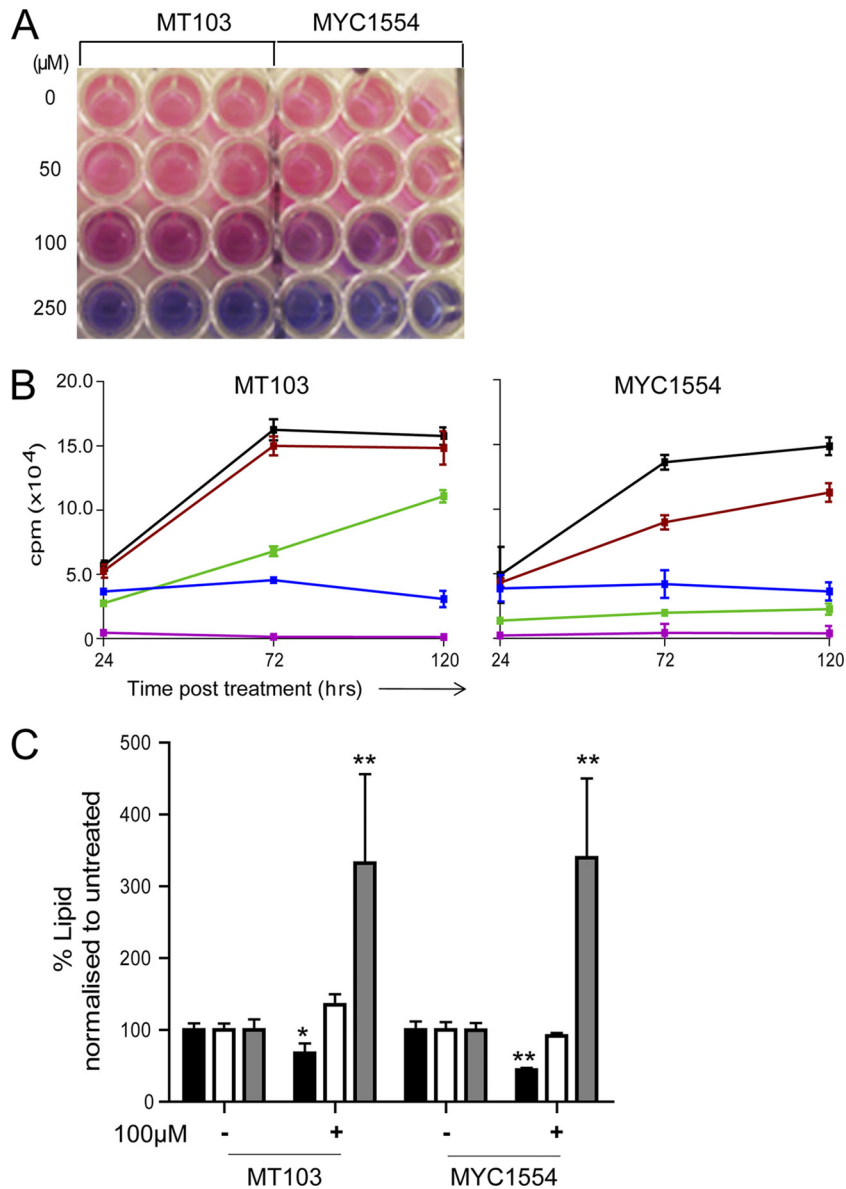


FIG 3 An Ag85C mutant is susceptible to I3-AG85 and displays a reduction of TDM upon I3-AG85 treatment. (A) Log-phase bacteria of an Ag85C mutant (MYC1554) and its wild-type background strain (MT103) were subjected to the indicated concentrations of I3-AG85 and tested with the standard resazurin assay. The figure is representative of two independent experiments. (B) Log-phase MYC1554 and MT103 bacteria were incubated with 50 μM (magenta), 100 μM (green), or 250 μM (pink) of I2-AG85, I3-AG85, or I4-AG85, with isoniazid (INH) at 10 μM (blue), or without compound (black), in 7H9 medium without detergent for 120 h. [^3H]uracil incorporation by *M. tuberculosis* was measured as described in the text. cpm is plotted against duration of exposure. Means \pm standard deviations from sextuplicates in a representative experiment from two independent experiments are shown. (C) Log-phase *M. tuberculosis* bacilli were treated with 100 μM I3-AG85 or left untreated and pulsed with [^{14}C]acetate to label lipids. Extractable lipids were resolved by thin-layer chromatography. TDM (black bars), TMM (white bars), and free mycolic acid (gray bars) band intensities were measured and normalized to total lane intensity. This was then converted to a percentage, with the value for the untreated sample taken as 100%. Each graph represents the means \pm standard deviations for duplicates in a representative experiment from two independent experiments. Statistical significance was calculated with the paired Student *t* test: *, $P < 0.05$; **, $P < 0.01$; ***, $P < 0.001$.

validated Ag85 as a drug target by detailed characterization of an Ag85C binding molecule, 2-amino-6-propyl-4,5,6,7-tetrahydro-1-benzothiophene-3-carbonitrile (I3-AG85). Derived from 2-amino-cyclohepta[*b*]thiophene-3-carbonitrile (I1-AG85), I3-AG85 exhibited antimycobacterial activity toward *M. tuberculosis* growing in broth culture and within macrophages.

Although chemical inhibitors against Ag85 proteins with activity toward other mycobacterial strains have been designed and tested, clear demonstration of pathway inhibition in *M. tubercu-*

losis is missing. We show that I3-AG85 blocks Ag85-mediated TDM synthesis with accumulation of the substrate, TMM, in *M. tuberculosis*. However, synthesis of covalently linked mycolic acids remains unaffected. A possible explanation for this might be conformational changes at the active site for arabinogalactan transfer of mycolic acid, which is inaccessible to I3-AG85. The three-dimensional (3D) structure of Ag85C cocrystallized with I3-AG85 could support this hypothesis. The highly conserved catalytic and sugar binding sites of Ag85 proteins should enable simultaneous

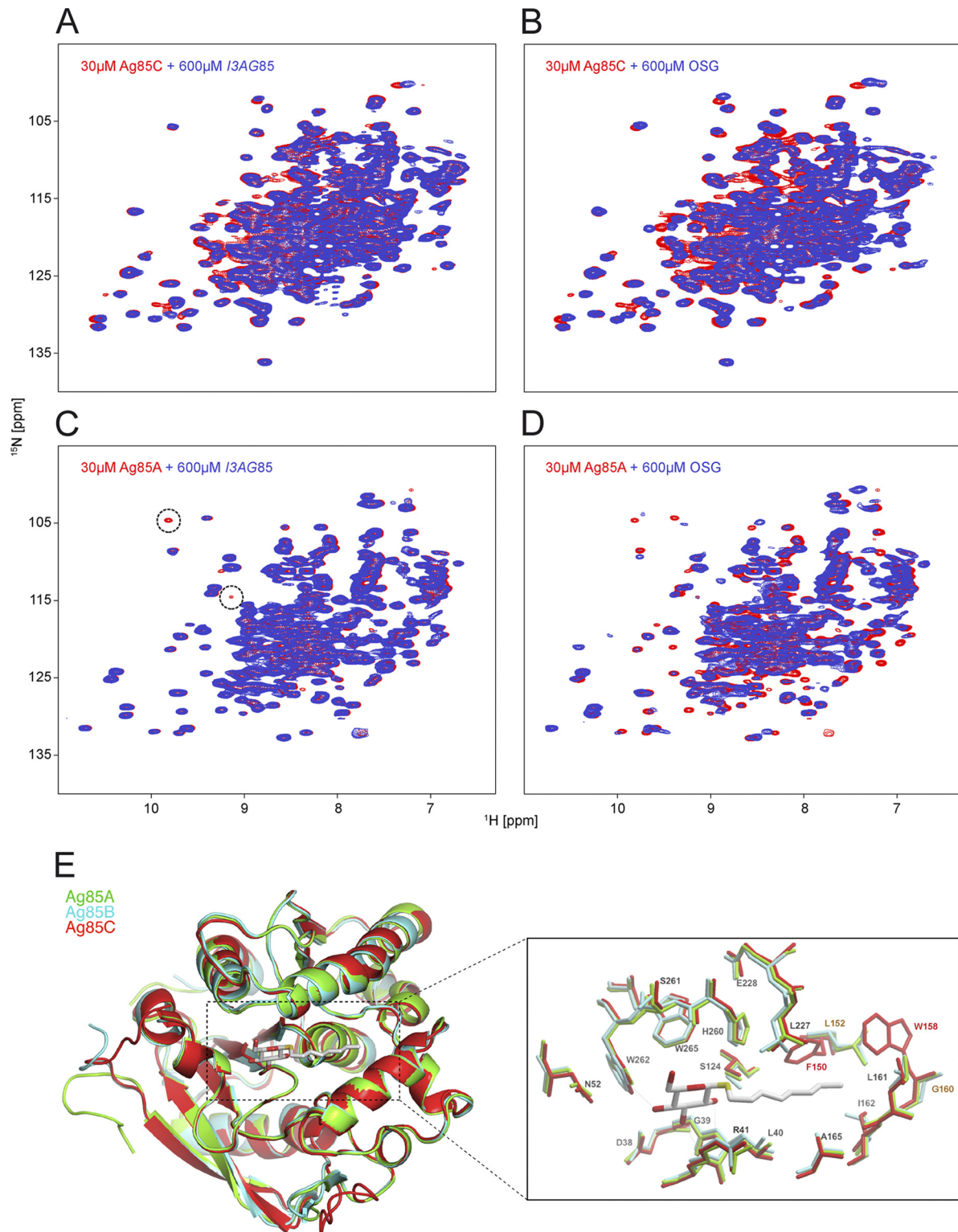


FIG 4 I3-AG85 binds only to Ag85C in the Ag85 family as revealed by NMR analysis. (A and B) Overlay of nuclear magnetic resonance (NMR) spectra of 30 μ M Ag85C with and without a 20-fold excess of I3-AG85 (A) and of 30 μ M Ag85C with and without a 20-fold excess of octylthioglucoiside (OSG) (B) in 5 mM citrate buffer (pH 6.0)–1 mM dithiothreitol (DTT)–0.1% CHAPS with 0.5% dimethyl sulfoxide (DMSO). (C and D) Analogous representations for Ag85A. Panels B and D indicate a clear pattern of binding of the artificial substrate OSG to Ag85C and Ag85A, respectively, by chemical shift changes. Panels A and C show less clear binding effects of I3-AG85 on Ag85C and Ag85A, respectively. While Ag85C showed a few chemical shift changes via interaction with I3-AG85 (A), the 15 N HSQC of Ag85A was nearly unchanged by this compound; only line broadening, which appeared to be a decrease in cross-peak intensity up to extinction (circles in panel C), was found. (E) OSG binding site in Ag85C (red). Structural superposition of Ag85A (green, 1SFR), Ag85B (blue, 1F0N) and Ag85C (red, 1VA5) is shown. Residues are numbered in black according to the Ag85C sequence. Residues labeled in brown correspond to positions in Ag85A/B that differ from those in Ag85C (red) (F150/L152 and W158/G160 in Ag85C and Ag85A/B, respectively). The catalytic triad is 100% identical (S124, H260, and E228) in all three Ag85 proteins. The surface residues that form the carbohydrate binding portion of substrate binding site are also 100% conserved in all three Ag85 proteins. In the mycolate binding site, F150 and W158 are present only in Ag85C (L152 and G160 in Ag85A and Ag85B).

inhibition of the three cognates through chemical blockade of the active site. Our analysis of I3-AG85 specificity through NMR binding assays and mutant susceptibility testing indicates a more complex scenario. The Ag85C mutant was susceptible to I3-AG85 treatment and displayed a reduced TDM phenotype, similar to wild type, hinting at simultaneous Ag85 protein family inhibition. However, NMR analysis did not detect significant binding of I3-AG85 to Ag85A or Ag85B. We observed only minor disturbance of Ag85A NMR signals by I3-AG85 and no effect on Ag85B signals. One possible explanation could simply be differential enzymatic activity of recombinant Ag85 proteins used *in vitro* for NMR experiments compared to their native counterparts in a complex *in vivo* environment used for MIC determination and lipid analysis. I3-AG85 could, for instance, interfere with alternate sites of the multiprotein Ag85 complex *in vivo* or cause allosteric effects when binding to the catalytic center of Ag85C. Such scenarios were not fully addressed when analyzing single purified recombinant proteins by NMR. Multidimensional interactions between Ag85 proteins are required for catalysis. Moreover, repression by feedback loops, involving products and precursors, might be involved. The slightly different substrate binding sites of Ag85C on the one hand and Ag85A and -B on the other lead to different activity profiles. The mild TDM synthase activity of Ag85A or -B, or any other vital process, could be repressed in wild-type strains due to allosteric effects or the accumulation of certain reactants and precursors (Fig. 2A). The survival of the Ag85C mutant could, for example, be attributed to the altered concentrations of mycolic acid derivatives (Fig. 3C) or a distinct topology of the remaining Ag85A-B complex lacking regulatory mechanisms present in the wild-type strain. Further experiments with more specific I3-AG85 derivatives would be useful to clarify the molecular basis of our observations.

The partial redundancy of Ag85A, -B, and -C, demonstrated through single-gene deletion and structural analysis, has added one more layer of complexity to our understanding of the distinct roles of cognates. The relatively high MIC of 100 μM (22 $\mu\text{g}/\text{ml}$) might prevent I3-AG85 from further development, but it could be a useful tool compound to dissect the Ag85-catalyzed pathway. Although phosphorylation of key enzymes, such as InhA, MabA, HadAB, and HadBC, has been identified as a regulatory mechanism to control mycolic acid synthesis, other mechanisms are possible (27, 43, 51). Thus, I3-AG85 could serve as a tool to identify novel regulatory pathways and the interdependence, if any, of overall lipid metabolic pathways in *M. tuberculosis*.

Additionally, I3-AG85 disrupts mycolic acid synthesis at a step distinct from that of the first-line drug INH, since the total mycolic acid abundance remained unchanged after I3-AG85 exposure. This can be presumably extended to other front-line drugs with the observed susceptibility of MDR and XDR *M. tuberculosis* strains to I3-AG85. Thus, the Ag85 pathway offers valuable targets that might overcome resistance to most, if not all, existing anti-TB drugs.

In conclusion, the Ag85 family of proteins, and thus mycolyl transferase activity, is a valid target for current TB drug discovery aiming to control MDR and XDR TB. Several front-runners in current clinical and preclinical studies, such as TMC-207, PA-824, and benzothiazinones, have a novel mode of action (3, 24, 46). However, additional candidate/lead compounds need to be identified to compensate for high attrition rates in drug discovery

pipelines and to counteract the continuing emergence of drug resistance.

ACKNOWLEDGMENTS

T.W. was supported by a fellowship from the Max Planck Society. This work was supported by the German Federal Ministry of Education and Research (BMBF) "X-Mtb Structural Genomics" Network (no. 0312992C) and the European Commission's Framework Programme 7 "NATT" (HEALTH-F3-2008-222965).

We thank Natalja Erdmann (Leibniz Institut für Molekulare Pharmakologie [FMP]) for protein production, Peter Schmieder (FMP) for recording NMR spectra, and Benjamin Bardiaux (FMP) for Fig. 4E. We also thank Diane Schad (Max Planck Institute for Infection Biology) and Arne Linden (FMP) for help preparing the figures and Mary Lu Grossman for help preparing the manuscript. We acknowledge Brigitte Gicquel for the gift of the MYC1554 and Mt103 strains and Kris Huygens for the NP_338463.1 and NP_336393.1 plasmids.

REFERENCES

1. Abou-Zeid C, et al. 1988. Characterization of fibronectin-binding antigens released by *Mycobacterium tuberculosis* and *Mycobacterium bovis* BCG. *Infect. Immun.* 56:3046–3051.
2. Anderson DH, Harth G, Horwitz MA, Eisenberg D. 2001. An interfacial mechanism and a class of inhibitors inferred from two crystal structures of the *Mycobacterium tuberculosis* 30 kDa major secretory protein (antigen 85B), a mycolyl transferase. *J. Mol. Biol.* 307:671–681.
3. Andries K, et al. 2005. A diarylquinoline drug active on the ATP synthase of *Mycobacterium tuberculosis*. *Science* 307:223–227.
4. Armitige LY, Jagannath C, Wanger AR, Norris SJ. 2000. Disruption of the genes encoding antigen 85A and antigen 85B of *Mycobacterium tuberculosis* H37Rv: effect on growth in culture and in macrophages. *Infect. Immun.* 68:767–778.
5. Austin PE, McCulloch EA, Till JE. 1971. Characterization of the factor in L-cell conditioned medium capable of stimulating colony formation by mouse marrow cells in culture. *J. Cell. Physiol.* 77:121–134.
6. Banerjee A, et al. 1994. inhA, a gene encoding a target for isoniazid and ethionamide in *Mycobacterium tuberculosis*. *Science* 263:227–230.
7. Barry CE, Crick DC, McNeil MR. 2007. Targeting the formation of the cell wall core of *M. tuberculosis*. *Infect. Disord. Drug Targets* 7:182–202.
8. Belisle JT, et al. 1997. Role of the major antigen of *Mycobacterium tuberculosis* in cell wall biogenesis. *Science* 276:1420–1422.
9. Benitez P, Medoff G, Kobayashi GS. 1974. Rapid radiometric method of testing susceptibility of mycobacteria and slow-growing fungi to antimicrobial agents. *Antimicrob. Agents Chemother.* 6:29–33.
10. Besra GS. 1998. Preparation of cell wall fractions from *Mycobacteria*, p 91–107. *In* Parish T, Stoker NG (ed), *Mycobacteria protocols*. Humana Press, Totowa, NJ.
11. Bodenhausen G, Ruben DJ. 1980. Natural abundance nitrogen-15 NMR by enhanced heteronuclear spectroscopy. *Chem. Phys. Lett.* 69:185–189.
12. Boucau J, Sanki AK, Voss BJ, Sucheck SJ, Ronning DR. 2009. A coupled assay measuring *Mycobacterium tuberculosis* antigen 85C enzymatic activity. *Anal. Biochem.* 385:120–127.
13. Connolly LE, Edelstein PH, Ramakrishnan L. 2007. Why is long-term therapy required to cure tuberculosis? *PLoS Med.* 4:e120.
14. Content J, et al. 1991. The genes coding for the antigen 85 complexes of *Mycobacterium tuberculosis* and *Mycobacterium bovis* BCG are members of a gene family: cloning, sequence determination, and genomic organization of the gene coding for antigen 85-C of *M. tuberculosis*. *Infect. Immun.* 59:3205–3212.
15. Copenhaver RH, et al. 2004. A mutant of *Mycobacterium tuberculosis* H37Rv that lacks expression of antigen 85A is attenuated in mice but retains vaccino-genic potential. *Infect. Immun.* 72:7084–7095.
16. Cosma CL, Sherman DR, Ramakrishnan L. 2003. The secret lives of the pathogenic mycobacteria. *Annu. Rev. Microbiol.* 57:641–676.
17. Daffé M, Reyat J-M. 2008. *The mycobacterial cell envelope*. ASM Press, Washington, DC.
18. Draper P. 1998. The outer parts of the mycobacterial envelope as permeability barriers. *Front. Biosci.* 3:D1253–D1261.
19. Elamin AA, Stehr M, Oehlmann W, Singh M. 2009. The mycolyltransferase 85A, a putative drug target of *Mycobacterium tuberculosis*: devel-

- opment of a novel assay and quantification of glycolipid-status of the mycobacterial cell wall. *J. Microbiol. Methods* 79:358–363.
20. Gobec S, et al. 2007. Design, synthesis, biochemical evaluation and antimycobacterial action of phosphonate inhibitors of antigen 85C, a crucial enzyme involved in biosynthesis of the mycobacterial cell wall. *Eur. J. Med. Chem.* 42:54–63.
 21. Jackson M, et al. 1999. Inactivation of the antigen 85C gene profoundly affects the mycolate content and alters the permeability of the Mycobacterium tuberculosis cell envelope. *Mol. Microbiol.* 31:1573–1587.
 22. Kremer L, Maughan WN, Wilson RA, Dover LG, Besra GS. 2002. The *M. tuberculosis* antigen 85 complex and mycolyltransferase activity. *Lett. Appl. Microbiol.* 34:233–237.
 23. Laneelle M-A, Daffe M. 2008. Transport assays and permeability in pathogenic mycobacteria, p 143–151. *In* Parish T, Brown AC (ed), *Mycobacteria protocols*. Humana Press, Totowa, NJ.
 24. Makarov V, et al. 2009. Benzothiazinones kill Mycobacterium tuberculosis by blocking arabinan synthesis. *Science* 324:801–804.
 25. Marrakchi H, Laneelle G, Quemard A. 2000. InhA, a target of the anti-tuberculous drug isoniazid, is involved in a mycobacterial fatty acid elongation system, FAS-II. *Microbiology* 146:289–296.
 26. Martin A, Camacho M, Portaels F, Palomino JC. 2003. Resazurin microtiter assay plate testing of Mycobacterium tuberculosis susceptibilities to second-line drugs: rapid, simple, and inexpensive method. *Antimicrob. Agents Chemother.* 47:3616–3619.
 27. Molle V, et al. 2010. Phosphorylation of InhA inhibits mycolic acid biosynthesis and growth of *Mycobacterium tuberculosis*. *Mol. Microbiol.* 78:1591–1605.
 28. Mori S, Abeygunawardana C, Johnson MO, van Zijl PC. 1995. Improved sensitivity of HSQC spectra of exchanging protons at short inter-scan delays using a new fast HSQC (FHSQC) detection scheme that avoids water saturation. *J. Magn. Reson. B* 108:94–98.
 29. Mosmann T. 1983. Rapid colorimetric assay for cellular growth and survival: application to proliferation and cytotoxicity assays. *J. Immunol. Methods* 65:55–63.
 30. Nathan C, et al. 2008. A philosophy of anti-infectives as a guide in the search for new drugs for tuberculosis. *Tuberculosis (Edinb.)* 88(Suppl. 1):S25–S33.
 31. Palomino JC, et al. 2002. Resazurin microtiter assay plate: simple and inexpensive method for detection of drug resistance in Mycobacterium tuberculosis. *Antimicrob. Agents Chemother.* 46:2720–2722.
 32. Piotto M, Saudek V, Sklenar V. 1992. Gradient-tailored excitation for single-quantum NMR spectroscopy of aqueous solutions. *J. Biomol. NMR* 2:661–665.
 33. Puech V, et al. 2002. Evidence for a partial redundancy of the fibronectin-binding proteins for the transfer of mycoloyl residues onto the cell wall arabinogalactan termini of Mycobacterium tuberculosis. *Mol. Microbiol.* 44:1109–1122.
 34. Raviglione MC, Smith IM. 2007. XDR tuberculosis—implications for global public health. *N. Engl. J. Med.* 356:656–659.
 35. Ronning DR, et al. 2000. Crystal structure of the secreted form of antigen 85C reveals potential targets for mycobacterial drugs and vaccines. *Nat. Struct. Biol.* 7:141–146.
 36. Ronning DR, Vissa V, Besra GS, Belisle JT, Sacchettini JC. 2004. Mycobacterium tuberculosis antigen 85A and 85C structures confirm binding orientation and conserved substrate specificity. *J. Biol. Chem.* 279:36771–36777.
 37. Rose JD, et al. 2002. Synthesis and biological evaluation of trehalose analogs as potential inhibitors of mycobacterial cell wall biosynthesis. *Carbohydr Res.* 337:105–120.
 38. Russell DG. 2007. Who puts the tubercle in tuberculosis? *Nat. Rev. Microbiol.* 5:39–47.
 39. Scheich C, Puetter V, Schade M. 2010. Novel small molecule inhibitors of MDR Mycobacterium tuberculosis by NMR fragment screening of antigen 85C. *J. Med. Chem.* 53:8362–8367.
 40. Schneider T, Sahl HG. An oldie but a goodie—cell wall biosynthesis as antibiotic target pathway. *Int. J. Med. Microbiol.* 300:161–169.
 41. Schon T, et al. 2009. Evaluation of wild-type MIC distributions as a tool for determination of clinical breakpoints for Mycobacterium tuberculosis. *J. Antimicrob. Chemother.* 64:786–793.
 42. Sheno S, Friedland G. 2009. Extensively drug-resistant tuberculosis: a new face to an old pathogen. *Annu. Rev. Med.* 60:307–320.
 43. Slama N, et al. 2011. Negative regulation by Ser/Thr phosphorylation of HadAB and HadBC dehydratase from *Mycobacterium tuberculosis* type II fatty acid synthase system. *Biochem. Biophys. Res. Commun.* 412:401–406.
 44. Smith CV, Sharma V, Sacchettini JC. 2004. TB drug discovery: addressing issues of persistence and resistance. *Tuberculosis (Edinb.)* 84:45–55.
 45. Stewart GR, Robertson BD, Young DB. 2003. Tuberculosis: a problem with persistence. *Nat. Rev. Microbiol.* 1:97–105.
 46. Stover CK, et al. 2000. A small-molecule nitroimidazopyran drug candidate for the treatment of tuberculosis. *Nature* 405:962–966.
 47. Takayama K, Kilburn JO. 1989. Inhibition of synthesis of arabinogalactan by ethambutol in Mycobacterium smegmatis. *Antimicrob. Agents Chemother.* 33:1493–1499.
 48. Takayama K, Wang C, Besra GS. 2005. Pathway to synthesis and processing of mycolic acids in Mycobacterium tuberculosis. *Clin. Microbiol. Rev.* 18:81–101.
 49. Takayama K, Wang L, David HL. 1972. Effect of isoniazid on the in vivo mycolic acid synthesis, cell growth, and viability of Mycobacterium tuberculosis. *Antimicrob. Agents Chemother.* 2:29–35.
 50. van den Boogaard J, Kibiki GS, Kisanga ER, Boeree MJ, Aarnoutse RE. 2009. New drugs against tuberculosis: problems, progress, and evaluation of agents in clinical development. *Antimicrob. Agents Chemother.* 53:849–862.
 51. Veyron-Churlet R, Zanelle-Cleon I, Cohen-Gonsaud Molle V, Kremer L. 2010. Phosphorylation of the Mycobacterium tuberculosis beta-ketoacyl-acyl carrier protein reductase MabA regulates mycolic acid biosynthesis. *J. Biol. Chem.* 285:12714–12725.
 52. von Kries JP, Warrier T, Podust LM. 2010. Identification of small-molecule scaffolds for p450 inhibitors. *Curr. Protoc. Microbiol.* Chapter 17:Unit17.4.
 53. Wang J, et al. 2004. Synthesis of trehalose-based compounds and their inhibitory activities against Mycobacterium smegmatis. *Bioorg. Med. Chem.* 12:6397–6413.
 54. World Health Organization. 2009. Global tuberculosis control: epidemiology, planning, financing: WHO report 2009. World Health Organization, Geneva, Switzerland.